

A computed line list for the H_2D^+ molecular ion

Taha Sochi* and Jonathan Tennyson†

Department of Physics and Astronomy, University College London, Gower Street, London WC1E 6BT, UK

Accepted —. Received —; in original form —

ABSTRACT

A comprehensive, calculated line list of frequencies and transition probabilities for the singly deuterated isotopologue of H_3^+ , H_2D^+ , is presented. The line list, called ST1, contains over 22 million rotational-vibrational transitions occurring between more than 33 thousand energy levels; it covers frequencies up to 18500 cm^{-1} . All energy levels with rotational quantum number, J , up to 20 are considered, making the line list useful for temperatures up to at least 3000 K. About 15% of these levels are fully assigned with approximate rotational and vibrational quantum numbers. The list is calculated using a previously proposed, high accuracy, *ab initio* model and consistency checks are carried out to test and validate the results. These checks confirm the accuracy of the list. A temperature-dependent partition function, valid over a more extended temperature range than those previously published, and cooling function are presented. Temperature-dependent synthetic spectra in the frequency range $0 - 10000\text{ cm}^{-1}$ are also given.

Key words: molecular spectra, discrete variable representation, H_2D^+ , infrared, rotation-vibration transitions, line list, partition function, cooling function.

1 INTRODUCTION

H_2D^+ is one of the simplest polyatomic quantum systems. It consists of two electrons bound to three nuclei (two protons and one deuteron) forming a triangular shape at equilibrium. The molecule is an asymmetric prolate top with three vibrational modes: breathing (ν_1), bending (ν_2) and asymmetric stretch (ν_3). All these modes are infrared active. H_2D^+ also possesses a permanent electric dipole moment of about 0.6 D due to the displacement of the center of charge from the center of mass. Hence pure rotational transitions, which occur in the far infrared, can occur. This all contrasts strongly with the non-deuterated H_3^+ molecular ion which has no allowed rotational spectrum and only one infrared active vibrational mode.

In astrophysical environments, H_2D^+ is formed by several reactions; the main one is



As this and other similar formation reactions are exothermic, the formation of H_2D^+ in the cold interstellar environment is favored. Consequently, the abundance of this species can be greatly enhanced compared to the underlying D/H ratio. As an isotopologue of H_3^+ , H_2D^+ is a major participant in chemical reactions taking place in interstellar medium. In particular, it plays a key role in the deuteration processes in

these environments (Millar 2003). Because H_3^+ lacks a permanent dipole moment and hence cannot be detected via radio astronomy, its asymmetrical isotopomers, namely H_2D^+ and D_2H^+ , are the most promising tracers of the extremely cold and highly dense interstellar clouds. These species are the last to remain in gaseous state under these extreme conditions with observable pure rotational spectra (Dalgarno *et al* 1973; Herbst and Millar 2008). Of these two isotopomers, H_2D^+ is the more abundant and easier to observe and hence it is the main species to utilize in such astrophysical investigations.

Although the existence of H_2D^+ in the interstellar medium (ISM) and astrophysical objects was contemplated decades ago (Dalgarno *et al* 1973; van Dishoeck *et al* 1992) with some reported tentative sighting (Phillips *et al* 1985; Pagani *et al* 1992; Boreiko and Betz 1993), it is only relatively recently that the molecule was firmly detected in the ISM via one of its rotational transition lines (Stark *et al* 1999). There have been many subsequent astronomical studies of H_2D^+ spectra (Caselli *et al* 2003; Vastel *et al* 2004; Ceccarelli *et al* 2004; Stark *et al* 2004; Hogerheijde *et al* 2006; Harju *et al* 2006; Cernicharo *et al* 2007; Caselli *et al* 2008). In particular these spectra have been used to investigate the mid-plane of proto-planetary disks (Ramos *et al* 2007), the kinematics of the centers of pre-stellar cores (van der Tak *et al* 2005), and the suggestion of possible use as a probe for the presence of the hypothetical cloudlets forming the baryonic dark matter (Ceccarelli and Dominik 2006).

* E-mail: t.sochi@ucl.ac.uk

† E-mail: j.tennyson@ucl.ac.uk

Vibrational transitions of H_2D^+ have yet to be observed astronomically.

The potential importance of H_2D^+ spectroscopy for cosmology is obvious as it is a primordial molecular species which could have a considerable abundance in the early universe. In particular it has a potential role in the cooling of primordial proto-objects (Dubrovich 1993; Dubrovich and Lipovka 1995; Dubrovich and Partridge 2000; Galli and Palla 1998; Schleicher *et al* 2008). Its significance is highlighted by a number of studies which consider the role of H_2D^+ in spectral distortions of Cosmic Microwave Background Radiation and whether this can be used to determine the H_2D^+ and deuterium abundances at different epochs (Dubrovich and Lipovka 1995). Finally the H_2D^+ 372 GHz line has been considered as a probe for the presence of dark matter (Ceccarelli and Dominik 2006).

Due to its fundamental and astrophysical importance, H_2D^+ has been the subject of a substantial number of spectroscopic studies. The first successful spectroscopic investigation of H_2D^+ was carried out by Shy *et al* (1981) where nine rotational-vibrational transitions were measured in the infrared region between 1800 and 2000 cm^{-1} using Doppler-tuned fast-ion laser technique, but no specific spectroscopic assignments were made. This was followed by other spectroscopic investigations which include the observation and identification of the strong and highly-important rotational $1_{10} - 1_{11}$ transition line of ortho- H_2D^+ at 372 GHz by Bogy *et al* (1984) and Warner *et al* (1984). Amano and Hirao (2005) measured the frequency of the $1_{10} - 1_{11}$ line of H_2D^+ with improved accuracy, as well as the $3_{21} - 3_{22}$ line at 646.430 GHz. The three fundamental vibrational bands of the H_2D^+ ion were observed by Amano and Watson (1984), Amano (1985) and Foster *et al* (1986) using laser spectroscopy. Fárník *et al* (2002) measured transitions to overtones $2\nu_2$ and $2\nu_3$ and to combination $\nu_2 + \nu_3$ in jet-cooled H_2D^+ ions. Hlavenka *et al* (2006) measured second overtone transition frequencies of H_2D^+ using cavity ringdown absorption spectroscopy. Other spectroscopic investigations include those of Asvany *et al* (2007), who detected 20 lines using laser induced reaction techniques, and the recent work of Yonezu *et al* (2009), who reported precise measurement of the transition frequency of the H_2D^+ $2_{12} - 1_{11}$ line at 2.363 THz, alongside three more far-infrared lines of H_2D^+ , using tunable far-infrared spectrometry. However, none of these studies measured absolute line intensities, although the work of Fárník *et al* (2002) and Asvany *et al* (2007) give relative intensities.

Several synthetic, H_2D^+ line lists have been generated from *ab initio* calculations. Prominent examples include the line list of Miller *et al* (1989) and another one generated as part of the work reported by Asvany *et al* (2007). Miller *et al*'s list extends to rotational level $J = 30$ and covers all levels up to 5500cm^{-1} above the ground state. These lists were used in a number of studies for various purposes such as spectroscopic assignment of energy levels and transition lines from astronomical observations, and for computation of a low-temperature partition function (Sidhu *et al* 1992). The line lists also played an important role in motivating and steering the experimental and observational work in this field (Miller *et al* 1989; Asvany *et al* 2007). Nonetheless, the previous H_2D^+ line lists suffered from limitations that include low energy cut-off and the inclusion of a lim-

ited number of levels especially at high J . These limitations, alongside the development of high accuracy *ab initio* models of H_3^+ and its isotopologues, including H_2D^+ , by Polyansky and Tennyson (1999), provided the motivation to generate a more comprehensive and accurate line list. The intention is that the new list will both fill the previous gaps and provide data of better quality.

The line list, which we call ST1, consists of 22164810 transition lines occurring between 33330 rotational-vibrational levels. These are all the energy levels with rotational quantum number $J \leq 20$ and frequencies below 18500cm^{-1} . This line list can be seen as a companion to the H_3^+ line list of Neale *et al* (1996) which has been extensively used for astrophysical studies; although for reasons explained below, the ST1 line list is actually expected to be more accurate.

2 METHOD

Vibration-rotation calculations were performed using the DVR3D code of Tennyson *et al* (2004). The code calculates, among other things, wavefunctions, energy levels, transition lines, dipole moments, and transition probabilities. DVR3D uses an exact Hamiltonian, within the Born-Oppenheimer approximation, and requires potential energy and dipole surfaces to be supplied as input. In general, it is these which largely determine the accuracy of the resulting calculations (Polyansky *et al* 2003).

The vibrational stage of the DVR3D suite requires an accurate model for the variation of electronic potential as a function of nuclear geometry. Here we use the H_3^+ global potential surface of Polyansky *et al* (2000), which used the ultra-high accurate *ab initio* data of Cencek *et al* (1998) supplemented by extra data points; the surface was constrained at high energy by the data of Schinke *et al* (1980). We added the H_2D^+ adiabatic correction term fitted by Polyansky and Tennyson (1999) to this surface. We also employed Polyansky & Tennyson's vibrational mass scaling to allow for non-adiabatic corrections to the Born-Oppenheimer approximation: we used $\mu_{\text{H}} = 1.0075372\text{u}$ and $\mu_{\text{D}} = 2.0138140\text{u}$ for the vibrational atomic masses, and $\mu_{\text{H}} = 1.00727647\text{u}$ and $\mu_{\text{D}} = 2.01355320\text{u}$ for the rotational atomic masses. The accuracy of this model is assessed below.

Calculations were performed in Jacobi coordinates (r_1, r_2, θ) , where r_1 represents the diatom distance (H-H), r_2 is the separation of the D atom from the center of mass of the diatom, and θ is the angle between r_1 and r_2 . Radial basis functions of Morse oscillator type were used to model r_1 (Tennyson and Sutcliffe 1982), while spherical oscillators were used to model r_2 (Tennyson and Sutcliffe 1983). Following Polyansky and Tennyson (1999), the Morse parameters for r_1 were set to $r_e = 1.71$, $D_e = 0.10$ and $\omega_e = 0.0108$, with 20 Gauss-Laguerre grid points. Parameters of the spherical oscillator functions were set to $\alpha = 0.0$ and $\omega_e = 0.0075$ with 44 Gauss-Laguerre grid points, following extensive tests on convergence of the vibrational band origins. 36 Gauss-Legendre grid points were used to represent the angular motion. The final vibrational Hamiltonian matrix used was of dimension 2000.

In the rotation stage, the size of the Hamiltonian matrix, which is a function of J , was set to $1800(J+1)$ following

Table 1. Sample of the ST1 levels file. The columns from left to right are for: index of level in file, J , symmetry, index of level in block, frequency in cm^{-1} , v_1 , v_2 , v_3 , J , K_a , K_c . We used -2 to mark unassigned quantum numbers.

730	1	4	99	18265.61525	-2	-2	-2	1	1	0
731	1	4	100	18379.99989	-2	-2	-2	1	1	0
732	1	4	101	18499.05736	-2	-2	-2	1	1	0
733	2	1	1	131.63473	0	0	0	2	0	2
734	2	1	2	223.86306	0	0	0	2	2	0
735	2	1	3	2318.35091	0	1	0	2	0	2
736	2	1	4	2427.09231	0	1	0	2	2	0
737	2	1	5	2490.93374	0	0	1	2	1	2
738	2	1	6	3123.27957	1	0	0	2	0	2
739	2	1	7	3209.80678	1	0	0	2	2	0

tests on $J = 3$ and $J = 15$. These tests demonstrated that choosing sufficiently large values for the rotational Hamiltonian, although computationally expensive, is crucial for obtaining reliable results. Our aim was to obtain convergence to within 0.01 cm^{-1} for all rotation-vibration levels considered. Our tests suggest we achieved this except, possibly, for some of the highest lying levels. For these levels our basic model, and in particular our corrections to the Born-Oppenheimer approximation, are not reliable to this accuracy.

To compute the intensity of the vibration-rotation transitions, a dipole moment surface is required. We used the *ab initio* dipole surface of Röhse *et al* (1994) to calculate the components of the H_2D^+ dipole. In the DIPOLE3 module of DVR3D we set the number of Gauss-Legendre quadrature points used for evaluating the wavefunctions and dipole surface to 50; this choice is consistent with the requirement that this parameter should be slightly larger than the number of DVR points used to calculate the underlying wavefunctions.

The final ST1 line list consists of two main files: one for the levels and the other for the transitions. These two files are constructed and formatted according to the method and style of the BT2 water line list (Barber *et al* 2006). The total amount of CPU time spent in producing the ST1 list including preparation, convergence tests, and verifying the final results is about 8000 hours. We used the serial version of the DVR3D suite on PC platforms running Linux (Red Hat) operating system. Both 32- and 64-bit machines were used in this work although the final data were produced mainly on 64-bit machines due to the large memory requirement for the high- J calculations.

This variational nuclear motion procedure used for the calculations provides rigorous quantum numbers: J , ortho/para and parity p , but not the standard approximate quantum numbers in normal mode, rigid rotor notation. We hand labelled those levels for which such quantum numbers could be assigned in a fairly straightforward fashion. 5000 of these levels are fully designated with 3 rotational (J, K_a, K_c) and 3 vibrational (v_1, v_2, v_3) quantum numbers, while 341 levels are identified with rotational quantum numbers only. Some of these assignments are made as initial guess and hence should be treated with caution. Tables 1 and 2 present samples of the ST1 levels and transitions files respectively.

Table 2. Sample of the ST1 transitions file. The first two columns are for the indices of the two levels in the levels file, while the third column is for the A coefficients in s^{-1} .

30589	29553	7.99E-04
19648	18049	8.37E-03
8943	7423	5.55E-01
8490	7981	2.18E-03
20620	22169	6.91E-04
17613	15937	5.62E-03
13046	11400	1.15E-00
20639	20054	7.26E-03
14433	17117	2.49E-03
25960	28074	1.92E-03

Table 3. Main experimental data sources used to validate the ST1 list. Columns 2 and 3 give the number of data points and the frequency range of the experimental data respectively, while the last three columns represent the minimum, maximum, and standard deviation of discrepancies (i.e. observed minus calculated) in cm^{-1} between the ST1 and the experimental data sets.

Source	N	Range (cm^{-1})	Min.	Max.	σ
Shy <i>et al</i> (1981)	9	1837 – 1953	-0.014	0.116	0.052
Amano and Watson (1984)	27	2839 – 3179	-0.315	0.054	0.065
Amano (1985)	37	2839 – 3209	-0.024	0.054	0.019
Foster <i>et al</i> (1986)	73	1837 – 2603	-0.134	0.213	0.067
Fárník <i>et al</i> (2002)	8	4271 – 4539	0.046	0.172	0.050
Asvany <i>et al</i> (2007)	25	2946 – 7106	0.008	0.242	0.088

3 RESULTS AND VALIDATION

3.1 Comparison to Experimental and Theoretical Data

We made a number of comparisons between the ST1 line list and laboratory data found in the literature. This enabled us to validate our results. The main sources of laboratory measurements that we used in our comparisons are presented in Table 3. The table also gives statistical information about the discrepancy between our calculated line frequencies and their experimental counterparts. Table 4 presents a rather detailed account of this comparison for a sample data extracted from one of these data sets, specifically that of Asvany *et al* (2007). This table also contains a comparison of relative Einstein B coefficients between theoretical values from ST1 and measured values from Asvany *et al*. The theoretical values in this table are obtained from the calculated A coefficients using the relation

$$B_{lu} = \frac{(2J' + 1)c^3 A_{ul}}{(2J'' + 1)8\pi h\nu^3} \quad (2)$$

where A_{ul} and B_{lu} are the Einstein A and B coefficients respectively for transition between upper (u) and lower (l) states, J' and J'' are the rotational quantum numbers for upper and lower states, h is Planck's constant, and ν is the transition frequency.

As seen, the ST1 values agree with the measured coefficients of Asvany *et al* to within experimental error in all cases. Other comparisons to previous theoretical data, such as that of Polyansky and Tennyson (1999), were also made and the outcome was satisfactory in all cases.

Table 4. Comparison between measured (Asvany *et al* 2007) and calculated (ST1) frequencies and relative Einstein B coefficients for a number of transition lines of H_2D^+ . These coefficients are normalized to the last line in the table. The absolute B coefficients, as obtained from the A coefficients of ST1 list using Equation 2, are also shown in column 5 as multiples of 10^{14} and in units of str.s.kg^{-1} .

Transition		Freq. (cm^{-1})		Relative B		
Vib.	Rot.	Obs.	ST1	ST1	Obs.	ST1
(0,3,0)	$1_{10} \leftarrow 1_{11}$	6303.784	6303.676	8.05	0.29	0.29
(0,3,0)	$1_{01} \leftarrow 0_{00}$	6330.973	6330.850	8.59	0.32 ± 0.02	0.31
(0,2,1)	$0_{00} \leftarrow 1_{11}$	6340.688	6340.456	7.36	0.27 ± 0.03	0.27
(0,2,1)	$2_{02} \leftarrow 1_{11}$	6459.036	6458.794	9.17	0.35 ± 0.04	0.34
(0,2,1)	$1_{11} \leftarrow 0_{00}$	6466.532	6466.300	27.3	1.00	1.00

3.2 Partition Function

The partition function of a system consisting of an ensemble of particles in thermodynamic equilibrium is given by

$$z(T) = \sum_i (2J_i + 1) g_i e^{-\frac{E_i}{kT}} \quad (3)$$

where i is an index running over all energy states of the ensemble, E_i is the energy of state i above the ground level which has rotational angular momentum J_i , k is Boltzmann's constant, T is temperature, and g_i is the nuclear spin degeneracy factor which is 1 for para states and 3 for ortho ones.

Using the ST1 energy levels we calculated the partition functions of H_2D^+ for a range of temperatures and compared the results to those obtained by Sidhu *et al* (1992). Table 5 presents these results for a temperature range of 5 – 4000 K. The results are also graphically presented in Figure 1. The table and figure reveal that although our results and those of Sidhu *et al* agree very well at temperatures below 1200 K, they differ significantly at high temperatures and the deviation increases as the temperature rises. This can be explained by the fact that ST1 contains more energy levels which contribute increasingly at high temperatures. We therefore expect our partition function to be the more reliable one for $T > 1200$ K.

Using a Levenberg-Marquardt nonlinear curve-fitting routine, we fitted the ST1 partition function curve to a fifth order polynomial

$$z(T) = \sum_{i=0}^5 a_i T^i \quad (4)$$

in temperature and obtained the following coefficients for T in K:

$$\begin{aligned} a_0 &= -0.300315 \\ a_1 &= +0.094722 \\ a_2 &= +0.000571 \\ a_3 &= -3.24415 \times 10^{-7} \\ a_4 &= +2.01240 \times 10^{-10} \\ a_5 &= -1.94176 \times 10^{-14} \end{aligned} \quad (5)$$

This polynomial is not shown on Figure 1 because it is virtually identical to the ST1 curve.

Table 5. Partition functions of H_2D^+ for a number of temperatures as obtained from Sidhu *et al* (1992) and ST1 line lists.

$T(\text{K})$	Partition Function Sidhu	Partition Function ST1	$T(\text{K})$	Partition Function Sidhu	Partition Function ST1
5	1.00	1.00	800	347.58	347.53
10	1.01	1.01	900	426.24	426.24
20	1.07	1.28	1000	515.43	516.31
30	2.15	2.15	1200	731.43	737.61
40	3.46	3.46	1400	1004.25	1026.84
50	5.05	5.05	1600	1339.43	1401.52
60	6.82	6.82	1800	1738.89	1881.33
70	8.73	8.73	2000	2203.94	2487.98
80	10.76	10.76	2200	2735.31	3244.83
90	12.90	12.89	2400	3327.58	4176.19
100	15.12	15.12	2600	3983.83	5306.36
150	27.56	27.55	2800	4698.51	6658.69
200	42.03	42.02	3000		8254.62
300	76.49	76.46	3200		10112.90
400	117.48	117.44	3400		12249.00
500	164.51	164.53	3600		14674.90
600	218.11	217.98	3800		17398.90
700	278.66	278.58	4000		20425.60

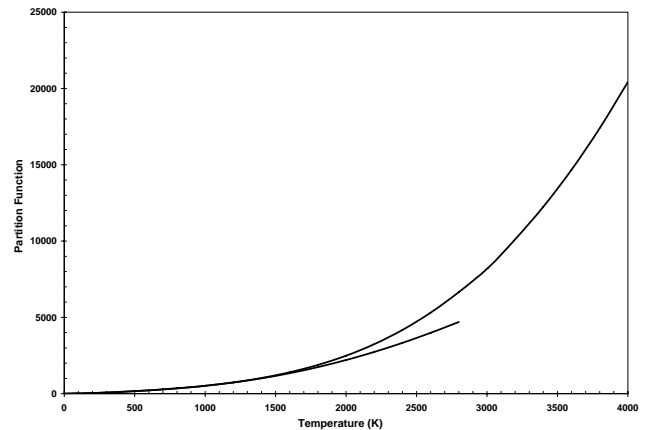


Figure 1. The H_2D^+ partition functions of ST1 (upper curve) and Sidhu *et al* (1992) (lower curve).

3.3 Cooling Function

ST1 was also used to compute the cooling function of H_2D^+ as a function of temperature. The cooling function W which quantifies the rate of cooling per molecule is given by

$$W(T) = \frac{1}{z} \left(\sum_{u,l} A_{ul} (E_u - E_l) (2J_u + 1) g_u e^{-\frac{E_u}{kT}} \right) \quad (6)$$

where u and l stand for the upper and lower levels respectively, and z is the partition function as given by Eq. 3. Figure 2 graphically presents our cooling function as a function of temperature alongside the H_3^+ cooling function of Neale *et al* (1996). As seen, the two curves are close for $T > 600$ K. However the H_2D^+ cooling function continues to be significant at lower temperatures, whereas at these temperatures the cooling curve of H_3^+ was not given by Neale *et al* (1996) because they considered it too small to be of significance.

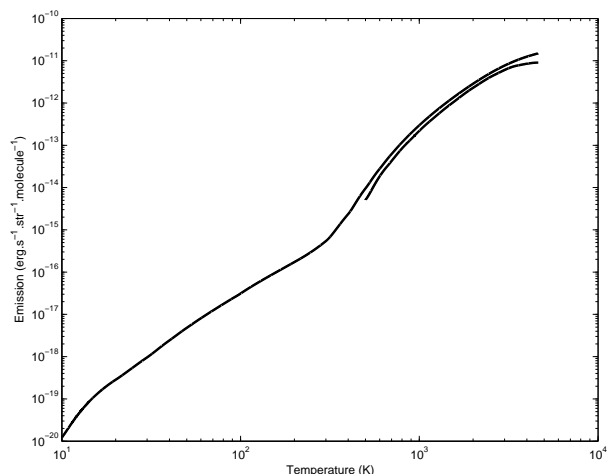


Figure 2. A graph of per molecule emission of H_2D^+ (upper curve) and H_3^+ (lower curve) as a function of temperature on a log-log scale. The H_2D^+ curve is obtained from ST1 while the H_3^+ curve is obtained from a digitized image from Neale *et al* (1996).

This is of course why the cooling properties of H_2D^+ could be important in the early universe.

Using a Levenberg-Marquardt curve-fitting routine, we fitted our H_2D^+ cooling function curve to a fourth order polynomial in temperature over the range 10 – 4000 K and obtained

$$W(T) = \sum_{i=0}^4 b_i T^i \quad (7)$$

$$\begin{aligned} b_0 &= -1.34302 \times 10^{-16} \\ b_1 &= +1.56314 \times 10^{-17} \\ b_2 &= -2.69764 \times 10^{-19} \\ b_3 &= +7.03602 \times 10^{-22} \\ b_4 &= -1.10821 \times 10^{-25} \end{aligned} \quad (8)$$

The fit was essentially perfect on a linear scale.

3.4 Synthetic Spectra

One of the main uses of line lists such as ST1 is to generate temperature-dependent synthetic spectra. We generated spectra from ST1 using the Spectra-BT2 code, which is described by Barber *et al* (2006) and is a modified version of the original spectra code of Tennyson *et al* (1993). Figure 3 (a) shows a temperature-dependent H_2D^+ absorption spectrum for the region largely associated with pure rotational transitions, while Figures 3 (b), (c) and (d) show the corresponding spectrum for the vibrational region. As is usual with rotation-vibration spectra, H_2D^+ spectra show a strong dependence on temperature.

4 CONCLUSIONS

In this study we present a new line list (ST1) for the triatomic ion H_2D^+ . The list, which can be obtained from the Centre de Données astronomiques de Strasbourg (CDS) database at <ftp://cdsarc.u-strasbg.fr/pub/cats/VI/130>,

comprises over 33 thousand rotational-vibrational energy levels and more than 22 million transition lines archived within two files. The tests performed on the line list suggest that, although it is based entirely on *ab initio* quantum mechanics, it should be accurate enough for almost all astronomical purposes. The one possible exception is for predicting the frequency of pure rotational transitions which are often needed to high accuracy and which are therefore better obtained from measured frequencies using combination differences.

5 ACKNOWLEDGEMENT

We thank Lorenzo Lodi for his help with the DVR3D code, and Steven Miller for encouraging to calculate H_2D^+ line list and for helpful discussions.

REFERENCES

- Amano T., Watson J.K.G., 1984, *J. Chem. Phys.*, 81, 2869
Amano T., 1985, *J. Opt. Soc. Am. B*, 2, 790
Amano T., Hirao T., 2005, *J. Mol. Spec.*, 233, 7
Asvany O., Hugo E., Müller F., Kühnemann F., Schiller S., Tennyson J., Schlemmer S., 2007, *J. Chem. Phys.*, 127, 154317-1
Barber R.J., Tennyson J., Harris G.J., Tolchenov R.N., 2006, *MNRAS*, 368, 1087
Bogey M., Demuynck C., Denis M., Destombes J.L., Lemoine B., 1984, *A&A*, 137, L15
Boreiko R.T., Betz A.L., 1993, *ApJ*, 405, L39
Caselli P., van der Tak F.F.S., Ceccarelli C., Bacmann A., 2003, *A&A*, 403, L37
Caselli P., Vastel C., Ceccarelli C., van der Tak F.F.S., Crapsi A., Bacmann A., 2008, *A&A*, 492, 703
Ceccarelli C., Dominik C., Lefloch B., Caselli P., Caux E., 2004, *ApJ*, 607, L51
Ceccarelli C., Dominik C., 2006, *ApJ*, 640, L131
Cencek W., Rychlewski J., Jaquet R., Kutzelnigg W., 1998, *J. Chem. Phys.*, 108, 2831
Cernicharo J., Polehampton E., Goicoechea J.R., 2007, *ApJ*, 657, L21
Dalgarno A., Herbst E., Novick S., Klemperer W., 1973, *ApJ*, 183, L131
Dubrovich V.K., 1993, *Astron. Lett.*, 19, 53
Dubrovich V.K., Lipovka A.A., 1995, *A&AT*, 296, 301
Dubrovich V., Partridge B., 2000, *A&AT*, 19, 233
Fárník M., Davis S., Kostin M.A., Polyansky O.L., Tennyson J., Nesbitt D.J., 2002, *J. Chem. Phys.*, 116, 6146
Foster S.C., McKellar A.R.W., Peterkin I.R., Watson J.K.G., Pan F.S., Crofton M.W., Altman R.S., Oka T., 1986, *J. Chem. Phys.*, 84, 91
Galli D., Palla F., 1998, *A&A*, 335, 403
Harju J., Haikala L.K., Lehtinen K., Juvela M., Mattila K., Miettinen O., Dumke M., Güsten R., Nyman L.-Å., 2006, *A&A*, 454, L55
Herbst E., Millar T.J., 2008, in Smith I.W.M., ed., *World Scientific Publishing*, ISBN: 978-1-84816-209-9, p. 1
Hlavenka P., Korolov I., Plašil R., Varju J., Kotrík T., Glofík J., 2006, *Czech. J. Phys.*, 56, B749

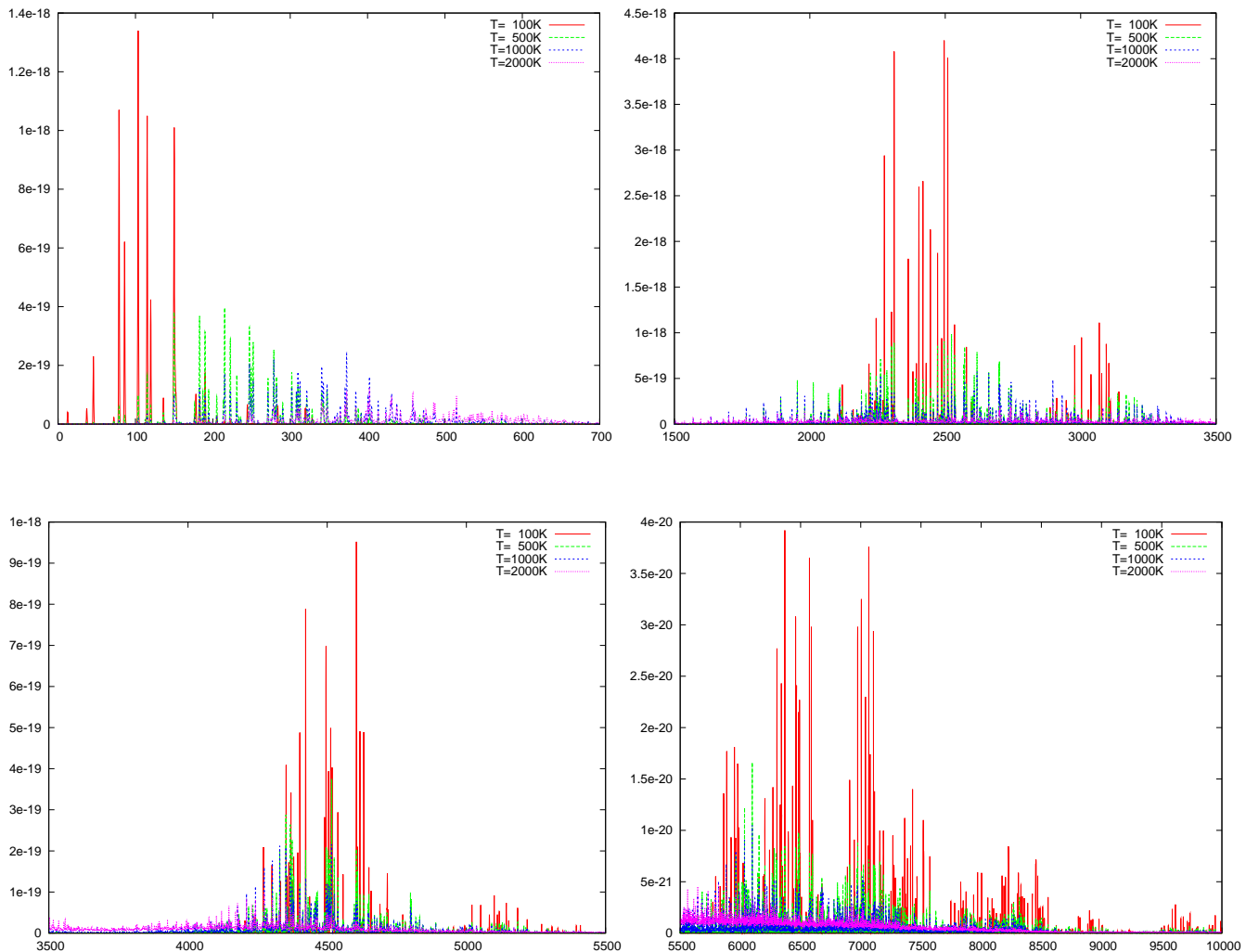


Figure 3. A graph of integrated absorption coefficient in $\text{cm}\cdot\text{molecule}^{-1}$ (on y axis) as a function of wave number in cm^{-1} (on x axis) within the range $0 - 10000 \text{ cm}^{-1}$ for $T = 100, 500, 1000$ and 2000 K .

Hogerheijde M.R., Caselli P., Emprechtinger M., van der Tak F.F.S., Alves J., Belloche A., Güsten R., Lundgren A.A., Nyman L.-Å., Volgenau N., Wiedner M.C., 2006, *A&A*, 454, L59

Millar T.J., 2003, *Space Sci. Rev.*, 106, 73

Miller S., Tennyson J., Sutcliffe B.T., 1989, *Mol. Phys.*, 66, 429

National Institute of Standards and Technology, URL: www.nist.gov

Neale L., Miller S., Tennyson J., 1996, *ApJ*, 464, 516

Pagani L., Wannier P.G., Frerking M.A., Kuiper T.B.H., Gulkis S., Zimmermann P., Encrenaz P.J., Whiteoak J.B., Destombes J.L., Pickett H.M., 1992, *A&A*, 258, 472

Phillips T.G., Blake G.A., Keene J., Woods R.C., Churchwell E., 1985, *ApJ*, 294, L45

Polyansky O.L., Tennyson J., 1999, *J. Chem. Phys.*, 110, 5056

Polyansky O.L., Prosimi R., Klopper W., Tennyson J., 2000, *Mol. Phys.*, 98, 261

Polyansky O.L., Császár A.G., Shirin S.V., Zobov N.F.,

Barletta P., Tennyson J., Schwenke D.W., Knowles P.J., 2003, *Science*, 299, 539

Ramos A.A., Ceccarelli C., Elitzur M., 2007, *A&A*, 471, 187

Röhse R., Kutzelnigg W., Jaquet R., Klopper W., 1994, *J. Chem. Phys.*, 101, 2231

Schinke R., Dupuis M., Lester W.A. Jr., 1980, *J. Chem. Phys.*, 72, 3909

Schleicher D.R.G., Galli D., Palla F., Camenzind M., Klessen R.S., Bartelmann M., Glover S.C.O., 2008, *A&A*, 490, 521

Shy J.-T., Farley J.W., Wing W.H., 1981, *Phys. Rev. A*, 24, 1146

Sidhu K.S., Miller S., Tennyson J., 1992, *A&A*, 255, 453

Stark R., van der Tak F.F.S., van Dishoeck E.F., 1999, *ApJ*, 521, L67

Stark R., Sandell G., Beck S.C., Hogerheijde M.R., van Dishoeck E.F., van der Wal P., van der Tak F.F.S., Schäfer F., Melnick G.J., Ashby M.L.N., de Lange G., 2004, *ApJ*, 608, 341

- Tennyson J., Sutcliffe B.T., 1982, *J. Chem. Phys.*, 77, 4061
Tennyson J., Sutcliffe B.T., 1983, *J. Mol. Spec.*, 101, 71
Tennyson J., Miller S., Le Sueur, C.R., 1993, *Comput. Phys. Commun.*, 75, 339
Tennyson J., Kostin M.A., Barletta P., Harris G.J., Polyansky O.L., Ramanlal J., Zobov N.F., 2004, *Comput. Phys. Commun.*, 163, 85
van der Tak F.F.S., Caselli P., Ceccarelli C., 2005, *A&A*, 439, 195
van Dishoeck E.F., Phillips T.G., Keene J., Blake G.A., 1992, *A&A*, 261, L13
Vastel C., Phillips T.G., Yoshida H., 2004, *ApJ*, 606, L127
Warner H.E., Conner W.T., Petrmichl R.H., Woods R.C., 1984, *J. Chem. Phys.*, 81, 2514
Yonezu T., Matsushima F., Moriwaki Y., Takagi K., Amano T., 2009, *J. Mol. Spec.*, 256, 238